PCA based Generalized Interpolation for Image Super-Resolution

C. V. Jiji and Subhasis Chaudhuri
Department of Electrical Engineering, Indian Institute of Technology-Bombay
Mumbai 400076. India
{ jiji, sc } @ ee.iitb.ac.in

Abstract

In this paper we propose an eigenimage based super-resolution reconstruction technique. Eigenimages of a database of several similar low resolution images are obtained and the given low resolution image is projected on to the eigenimages to compute the eigenimage coefficients. The eigenimages are then interpolated using any conventional interpolation method and approximated to the nearest orthonormal bases. The high resolution image is reconstructed using these bases and the same coefficients determined as above. This method is applicable to images of a particular class and results are demonstrated for both face and fingerprint images. The algorithm offers significant advantage when the input image is blurred and noisy.

1. Introduction

In most imaging applications, images with high spatial resolution are desired and often required. Resolution enhancement from a single observation using image interpolation techniques is of limited application because of the aliasing present in the low-resolution image. *Super-resolution* refers to the process of producing a high spatial resolution image than what is afforded by the physical sensor through post processing means. It includes up-sampling the image, thereby increasing the maximum spatial frequency, and removing degradations that arise during the image capture, viz., aliasing and blurring. In general, there are two classes of super-resolution techniques: reconstruction-based and learning-based. In reconstruction-based techniques the high resolution image is recovered from several low resolution observations of the input, but in learning-based super-resolution algorithms a database of several other images are used to obtain the high resolution image.

In many biometric databases, a large number of images of similar content, shape and size are available. For example, in investigative criminology one has available face and fingerprint databases. These are often taken at controlled environment. The question we ask is that if one encounters a poor quality input image, can it be enhanced using the knowledge of the properties of the database images ? Thus, the basic problem that we solve in this paper is as follows. Given a low resolution input image belonging to a particular class (face, fingerprint, etc.) and a database of several low resolution images of the same class, obtain a high resolution output. We perform principal component analysis (PCA) on the low resolution image database and an appropriate interpolation is carried out on the eigenimages, using which the high resolution image is reconstructed. We find this method particularly useful when the input image is noisy and partly blurred so that the other existing learning-based methods do not provide a good solution.

2. Related Work

Numerous reconstruction-based super-resolution algorithms have been proposed in the literature. The super-resolution idea was first proposed by Tsai and Huang that used the frequency domain approach [17]. A different approach to the super-resolution restoration problem was suggested by Irani *et al.* [7, 8] based on the iterative back projection method. Ng *et al.* develop a regularized, constrained total least squares solution to obtain a high-resolution image in [12]. A maximum *aposteriori* (MAP) estimator with Huber-Markov Random Field (MRF) prior is described by Schultz and Stevenson in [16]. Other approaches include a MAP-MRF based super-resolution technique using the blur as a cue [15]. In [14] the authors recover both the high resolution scene intensity and the depth fields simultaneously using the defocus cue. Elad and Feuer [3] proposed a unified methodology for super-resolution restoration from several geometrically warped, blurred, noisy and down-sampled measured images by combining maximum likelihood (ML), MAP and projection onto convex sets (POCS) approaches. Recently, Lin and Shum determine the quantitative limits of reconstruction-based super-resolution algorithms and obtain the up-sampling limits from the conditioning analysis of the coefficient matrix [11].

The ideas described in [1], [2], [4], [6] and [10] belong to the learning-based super-resolution category. In [4] Freeman *et al.* proposed a parametric Markov network to learn the statistics between the “scene” and the “image”, as a framework for handling low-level vision tasks, one application of which is super-resolution. Authors in [2] have proposed a super-resolution technique from multiple views using learnt image models making use of PCA. In [1] Baker and Kanade develop a super-resolution algorithm by modifying the prior term in the cost to include the results of a set of recognition decisions, and call it recognition based super-resolution or hallucination. Their prior enforces the condition that the gradient in the super-resolved image should be equal to the gradient in the best matching training image. In [9], we have proposed a single frame super-resolution algorithm using a wavelet based learning technique. An image analogy method applied to super-resolution is discussed in [6]. An eigenface-domain super-resolution reconstruction algorithm for face recognition is proposed in [5]. The face hallucination technique proposed in [19] is similar to our method, but here the authors make use of both low and high resolution image databases to recover the high resolution image. They also add constraints to the principal components to reduce the nonface-like distortion. The algorithm that we propose in this paper can be put under the category of learning-based super-resolution where we make use of only a low resolution image database to obtain the super-resolved image.

3. PCA-Based Interpolation

3.1. Low resolution image formation model

It is assumed that the observed low resolution image is produced from a single high resolution image under the following generative model. Let z represent the lexicographically ordered high resolution image of $N^2 \times 1$ pixels. If y is the $M^2 \times 1$ lexicographically ordered vector containing pixels from the low resolution observation, then it can be modeled as

$$y = DHz + n \tag{1}$$

where D is the decimation matrix, size of which depends on the decimation factor and H is the blur matrix. For a decimation factor of q, $N = qM$ and the decimation matrix D consists of q^2 non-zero elements of value $\frac{1}{q^2}$ along each row at appropriate locations and has the form [16] (using a proper reordering of z)

$$D = \frac{1}{q^2}\begin{bmatrix} 11\ldots1 & & & \mathbf{0} \\ & 11\ldots1 & & \\ & & \ddots & \\ \mathbf{0} & & & 11\ldots1 \end{bmatrix}. \tag{2}$$

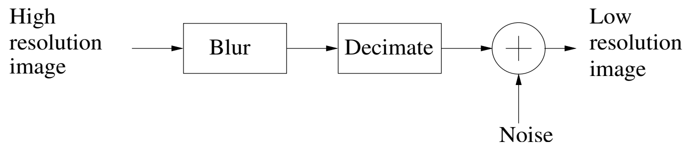

Figure 1. Illustration of low resolution image formation model.

As an example, for a decimation factor of $q = 2$ and with lexicographically ordered z of size, say 16×1, the D matrix is of size 4×16 and can be written as

$$D = \frac{1}{4}\begin{bmatrix} 1100110000000000 \\ 0011001100000000 \\ 0000000011001100 \\ 0000000000110011 \end{bmatrix}. \tag{3}$$

In equation (1), n is the $M^2 \times 1$ noise vector. We assume the noise to be zero mean but no specific distribution is assumed in this work. The low resolution image formation model is illustrated in Figure 1.

3.2. Eigen-image decomposition

An image can be reconstructed from eigen images in the PCA representation as described in [18]. The basic procedure for computing the eigen space is as follows: We have a dataset of K similar low-resolution images, represented by the matrix $[x_1, x_2, \ldots, x_K]$, where x_i is the i^{th} image vector. In PCA, a set of top k eigenvectors $E_l = [e_{1l}, e_{2l}, \ldots, e_{kl}]$, also called eigenimages, are computed from the covariance matrix,

$$C = \sum_{i=1}^{K}(x_i - m_x)(x_i - m_x)^T. \tag{4}$$

where m_x is the average image intensity defined by

$$m_x = \frac{1}{K}\sum_{i=1}^{K} x_i. \tag{5}$$

For a given low-resolution image y_l, a weight vector is computed by projecting it onto eigenimages,

$$w_l = {E_l}^T(y_l - m_x). \tag{6}$$

An approximation of y_l can be obtained from the top k eigenimages,

$$\hat{y}_l = E_l w_l + m_x. \tag{7}$$

Since k is typically much smaller than the size of the image vector, the image representation through the eigenimage expansion is not complete. Hence $\hat{y}_l$ is an approximation of y_l and the quality of approximation depends on its nearness to the class of images in the database.

3.3. Eigen-image interpolation

Now we wish to form a set of high resolution eigenimages using which we can construct the high resolution output corresponding to the given low resolution input image. In order to do this all the k low resolution eigenvectors and the mean vector are interpolated using the bicubic interpolation. Any other suitable interpolation scheme can also be used. But we restrict to bicubic interpolation in this study. The interpolated set of eigenvectors are given by $E_h = [e_{1h}, e_{2h}, \ldots, e_{kh}]$. One may use appropriate upsampling factor such as $q = 2, 3, 4$, etc. The new set of interpolated eigenvectors need not be orthonormal. They are then transformed into the nearest set of orthonormal vectors using the Gram-Schmidt orthogonalization procedure. Since all these vectors are of unit norm, the weights (eigen values associated with the corresponding eigenimages) must be multiplied by the upsampling factor q (i.e., $w_h = qw_l$) to preserve the covariance structure given in equation (4).

The high resolution image is now reconstructed using

$$\hat{z} = E_h w_h + m_z \tag{8}$$

where m_z is the high resolution mean vector obtained by interpolating the low resolution mean vector m_x.

Let us now discuss why the above operation performs a super-resolution restoration of a given input image. Since the eigenimage representation (see equation 7) is an incomplete representation and since the noise present in the input image is expected to be uncorrelated to all the available basis vectors, the reconstruction process reduces the noise drastically. Also, if the input image is blurred, it will still have significant correlation with the corresponding eigenimages of the *ideal* image. Since the eigenimages have been computed using the good quality training images, the reconstruction process is expected to remove the blur present in the data. Needless to say, if the input image is badly blurred, the associated eigen expansion may be very different from that of the ideal image, when the reconstruction will be very poor. Direct interpolation of the input image does not solve any of the above two problems of blurring and noise perturbation. However, we must mention that interpolation of individual eigenimages does not recover the high frequency details lost during the low resolution sampling process explained in equation (1). Hence no additional frequency details are recovered during the interpolation process. Under this argument, one can always say that the proposed method does not achieve an image super-resolution. But one does achieve image deblurring and noise removal.

4. Equivalence to generalized interpolation

The super-resolution method described as above is conceptually equivalent to the generalized interpolation scheme reported in [13] for image expansion and generation of super-resolution images. This is done by decomposing the image into appropriate subspaces, carrying out interpolation in individual subspaces and subsequently transforming the interpolated values back to the image domain. Consider a function $f(x,y)$ decomposed as

$$f(x,y) = g(a_1(x,y), a_2(x,y), \ldots, a_m(x,y)) \tag{9}$$

where $a_i(x,y)$, $i = 1, 2, \ldots, m$ are different functions of the interpolating variables x and y and when they are combined by an appropriate m-variate function g, one recovers the original function f. Now the individual functions $a_i(x,y)$ are interpolated and combined using equation(9) to obtain the rescaled function $f(x \uparrow q, y \uparrow q)$. In [13] photometric cues were used to decompose the image assuming a Lambertian reflectance model, and the interpolants were $a_1(x,y) = p(x,y)$, $a_2(x,y) = q(x,y)$ and $a_3(x,y) = \rho(x,y)$ where p and q are the surface normals and ρ is the albedo. It is to be noted that various optical and structural properties of the image, such as 3-D shape of an object, regional homogeneity, local variations in scene reflectivity, etc., can be better preserved during the interpolation process. It was also shown that an alias free reconstruction of $f(x \uparrow q, y \uparrow q)$ is possible if the subfunctions are all bandlimited.

In our case g is a linear function , i.e.,

$$g(a_1(x,y), a_2(x,y), \ldots, a_m(x,y)) = \sum_{i=1}^{m} w_i \bar{a}_i \tag{10}$$

where $\bar{a}_i$ corresponds to the principal components obtained from PCA decomposition. Here $\bar{a}_i$'s are orthogonal to each other and they are derived from the database images. Thus the proposed method is a special case of generalized interpolation.

5. The complete algorithm

The complete algorithm is summarized below in terms of the steps involved.

STEP 1:
Perform the PCA decomposition on the low resolution image database to get k eigenimages represented by the matrix E_l and also obtain the mean image m_x.
STEP 2:
Project the given low resolution image y_l onto the eigen images to get the eigenimage coefficients w_l.
STEP 3:
Interpolate the eigenimages and the mean image to get the corresponding high resolution eigenimage matrix E_h and the high resolution mean image m_z.
STEP 4:

Approximate the high resolution eigenimages to the nearest orthonormal bases.
STEP 5:
Obtain the super-resolved image using equation 8.

6. Experimental Results

Experiments were conducted on both face and fingerprint images. For face images the database consisted of 105 low resolution images of size 82×96 pixels. All the images were of frontal face and no pre-processing was done on them. A high resolution image is blurred using a 3×3 Gaussian kernel with standard deviation 0.5, downsampled and added with zero mean Gaussian noise of different standard deviations(σ) to form the input image.

Figure 2 shows the first 10 low resolution eigenimages computed from the database of 105 face images. In Figure 3 the noisy low resolution image with $\sigma = 0.1$ and the corresponding bicubic interpolated image and the super-resolved image for zoom factors of $2, 4$ and 5 are shown. It can be observed that the super-resolved image is almost noise free and more clear than the bicubic interpolated image which is highly noisy. In Figure 4, even though the low resolution observation is much more noisy ($\sigma = 0.5$), the super-resolved image is of far better quality compared to the bicubic interpolated image which is very noisy. This is also quantified in terms of the peak signal to noise ratio (PSNR) tabulated in table 1 where the PSNRs for the bicubic interpolated image and super-resolved image for a zoom factor 4 for different values of noise level are shown. As mentioned in Section 3.3 it is observed that when σ is very large the reconstructed image deviates from the original face image. In Figure 5(a) a low resolution input which is blurred with 7×7 Gaussian mask with standard deviation of 2 is shown. As expected, the bicubic output is heavily blurred, but the super-resolved image is almost free from blur. This demonstrates that as long as there is a good correlation of the input image with the eigenimages, a good reconstruction is, indeed, possible. It is also observed that when the low resolution input is free from noise the bicubic interpolated image appears to be slightly more blurred (observe the eyes) than the super-resolved image as can be seen from Figure 6. Thus the key aspect about our algorithm is its capability to recover a good quality super-resolved image when the low resolution input image is blurred and noisy. In all the above experiments 100 eigenimages were used to reconstruct the super-resolved image.

Now we experiment on how many eigenimages are required for a good reconstruction. Figure 7 shows the super-resolved image obtained using $10, 20$ and 50 eigen images($\sigma = 0.1, q = 4$). It is observed that using the top 50 eigenimages a good quality output can be reconstructed. In all the above experiments the low resolution input image was a part of the database which consisted of 75 male faces and 35 female faces. Figure 8 shows the bicubic interpolated image and the super-resolved image corresponding to an input face image which is not present in the database. In this case also we are able to obtain a better super-resolved image.

In the next experiment we demonstrate that if the input image does not belong to the class of images in the database, one cannot do any meaningful reconstruction. Figure 9 shows the reconstructed image for some arbitrary input image using the face image database and 100 eigenimages. Here the output is not at all related to the input which indicates clearly that the proposed method is applicable only for a class of images.

One of the drawbacks of PCA based analysis of images is that the image size should be same in all cases. We now demonstrate that how this can be circumvented. In Figure 10(a) a low resolution observation of size 41×48 pixels is shown. The database images were of dimension 82×96 pixels. Figure 10(b) shows the bicubic interpolated output for a zoom factor of 8. The low resolution input is first bicubic interpolated by a factor of 2 and then super-resolved by a factor of 4 using the proposed approach and the corresponding result is shown in 10(c). As expected, the super-resolved image is less blurred than the bicubic result. This technique can be adopted to get a good quality super resolved image when the input image size is very small or different from the database images.

We now show results of experiments on a different database. Figure 11 shows the low resolution input, bicubic interpolated results and the super-resolved images for zoom factors of 2, 4 and 5 for a fingerprint image. The results are shown for noise level $\sigma = 0.1$. It can be observed that the super-resolved image is more clear and noise free compared to the bicubic interpolated image. The PSNR for the bicubic interpolated image and the super-resolved for a zoom factor of 4 are compared in table 1 for different values of σ. In this experiment the low resolution database consisted of 150 fingerprint images of size 32×32 pixels, and the top 100 eigenimages were used for reconstruction.

7. Conclusions

We have described a method for super-resolution restoration of images of a particular class using a PCA based generalized interpolation technique. The low resolution eigenimages obtained from PCA decomposition are interpolated and transformed into an orthonormal basis to reconstruct the super-resolved image. The results obtained for both face and fingerprint images show far better perceptual as well as quantifiable improvements over conventional interpolation techniques. The proposed method is useful when multiple observations of the input are not available and one

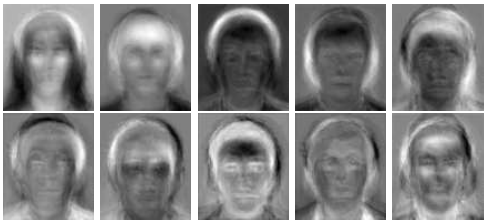

Figure 2. First ten eigenimages.

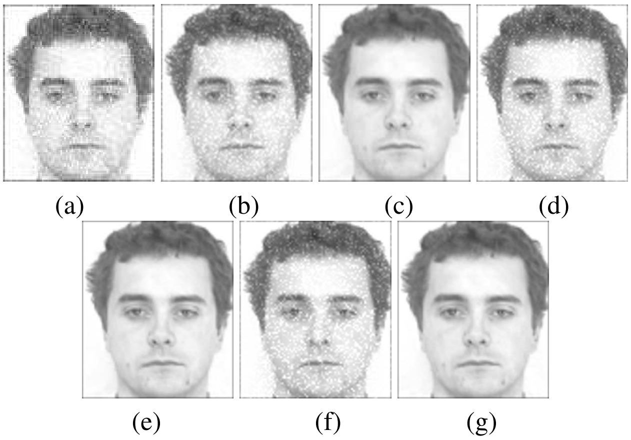

Figure 3. (a) A low resolution noisy observation ($\sigma = 0.1$) , (b)$\uparrow 2$ bicubic interpolated image, (c)$\uparrow 2$ super-resolved image, (d)$\uparrow 4$ bicubic interpolated image, (e)$\uparrow 4$ super-resolved image, (f) $\uparrow 5$ bicubic interpolated image and (g) $\uparrow 5$ super-resolved image. Here $\uparrow q$ defines the upsampling factor.

must make the best use of a poor quality single observation to enhance its resolution. In future, we plan to compare the performance of the proposed method with those of Baker and Kanade [1] and Freeman *et al.* [4].

References

[1] S. Baker and T. Kanade. Limits on Super-Resolution and How to Break Them. *IEEE Trans. on Pattern Analysis and Machine Intelligence*, 24(9):1167–1183, September 2002.

[2] D. Capel and A. Zisserman. Super-Resolution from Multiple Views using Learnt Image Models. In *Proc. IEEE Int. Conf. on Computer Vision and Pattern Recognition*, pages II:627–634, 2001.

[3] M. Elad and A. Feuer. Restoration of a Single Superresolution Image from Several Blurred, Noisy and Undersampled Measured Images. *IEEE Trans. on Image Processing*, 6(12):1646–1658, December 1997.

[4] W. T. Freeman, T.R.Jones, and E. C.Pasztor. Example-Based Super-Resolution. *IEEE Computer Graphics and Applications*, 22(2):56–65, March/April 2002.

[5] B. K. Gunturk, A. U. Batur, Y. Altunbasak, M. H. Hayes, and R. M. Mersereau. Eigenface-Domain Super-Resolution for Face Recognition. *IEEE Trans. on Image Processing*, 12(5):597–606, May 2003.

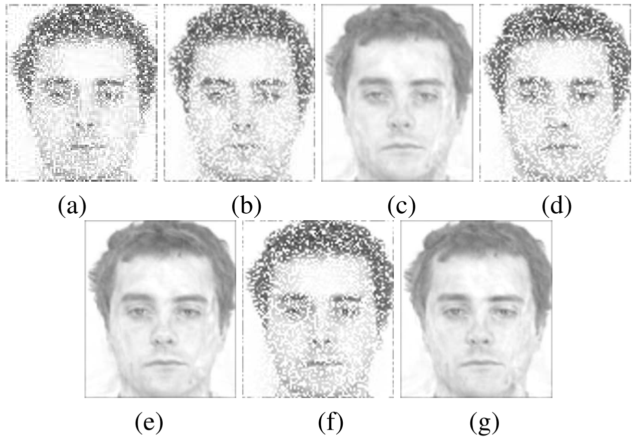

Figure 4. (a) A low resolution observation ($\sigma = 0.5$). Results of bicubic interpolation: (b) $q = 2$, (d) $q = 4$ and (f) $q = 5$. Super-resolved images: (c) $q = 2$, (e) $q = 4$ and (g) $q = 5$.

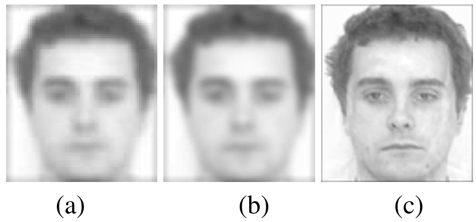

Figure 5. (a) A very blurred low resolution observation , (b)$\uparrow 4$ bicubic interpolated image and (c)$\uparrow 4$ super-resolved image.

Figure 6. (a) A good quality low resolution observation (noise free) , (b)$\uparrow 4$ bicubic interpolated image and (c) the $\uparrow 4$ super-resolved image using the proposed approach.

	Method	$\sigma = 0.1$	$\sigma = 0.2$	$\sigma = 0.5$
Face	Bicubic	22.93	20.27	16.78
	Proposed	24.23	22.88	19.79
Fingerprint	Bicubic	20.88	17.76	13.72
	Proposed	21.36	20.01	16.50

Table 1. Comparison of PSNRs for the zoom factor $q = 4$.

k=10 k=20 k=50

Figure 7. Super-resolution reconstructions using different numbers of eigenimages.

(a) (b) (c)

Figure 8. Super-resolution reconstruction for an input image not present in the database: (a) low resolution observation, (b) $\uparrow 4$ bicubic interpolated image and (c) $\uparrow 4$ super-resolved image.

(a) (b)

Figure 9. Super-resolution reconstruction for any arbitrary input image not belonging to the image class (a) low resolution input and (b) $\uparrow 4$ super-resolved image.

(a) (b) (c)

Figure 10. (a) A low resolution observation of different image size 41×48 pixels , (b)$\uparrow 8$ bicubic interpolated image and (c) super-resolved image.

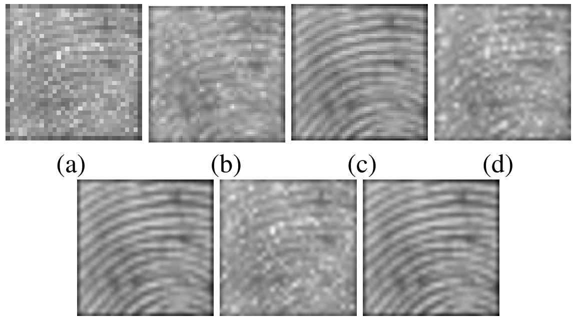

(a) (b) (c) (d)

(e) (f) (g)

Figure 11. (a) A low resolution poor quality fingerprint image. Results of bicubic interpolation: (b) $q = 2$, (d) $q = 4$ and (f) $q = 5$. Super-resolved images: (c) $q = 2$, (e) $q = 4$ and (g) $q = 5$.

[6] A. Hertzmann, C. E. Jacobs, N. Oliver, B. Curless, and D. H. Salesin. Image Analogies. In *Proc. SIGGRAPH*, pages 327–340, 2001.

[7] M. Irani and S. Peleg. Improving Resolution by Image Registration. *CVGIP:Graphical Models and Image Processing*, 53:231–239, March 1991.

[8] M. Irani and S. Peleg. Motion Analysis for Image Enhancement : Resolution, Occlusion, and Transparency. *VCIR*, 4:324–335, December 1993.

[9] C. V. Jiji, M. V. Joshi, and S. Chaudhuri. Single Frame Image Super-resolution Using Learnt Wavelet Coefficients. *International Journal of Imaging Systems and Technology*, (to appear).

[10] M. V. Joshi and S. Chaudhuri. A Learning-Based Method for Image Super-Resolution from Zoomed Observations. In *Proc. fifth Int. Conf. on Advances in Pattern Recognition*, pages 179–182, Indian Statistical Institute, Kolkata, India, 2003.

[11] Z. Lin and H. Y. Shum. Fundamental Limits of Reconstruction-Based Super-Resolution Algorithms under Local Translation. *IEEE Trans. on Pattern Analysis and Machine Intelligence*, 26(1):83–97, January 2004.

[12] M. K. Ng, N. K. Bose, and J. Koo. Constrained Total Least Squares Computation for High Resolution Image Reconstruction with Multisensors. *International Journal of Imaging Systems and Technology*, 12:35–42, 2000.

[13] D. Rajan and S. Chaudhuri. Generalized Interpolation and its Applications in Super-Resolution imaging. *Image and Vision Computing*, 19:957–969, November 2001.

[14] D. Rajan and S. Chaudhuri. Simultaneous Estimation of Super-Resolved Intensity and Depth Maps from Low Resolution Defocussed Observations of a Scene. In *Proc. IEEE Int. Conf. on Computer Vision*, pages 113–118, Vancouver Canada, 2001.

[15] D. Rajan and S. Chaudhuri. Generation of Super-resolution Images from Blurred Observations using an MRF Model. *J. Mathematical Imaging and Vision*, 16:5–15, 2002.

[16] R. R. Schultz and R. L. Stevenson. A Bayesian Approach to Image Expansion for Improved Definition. *IEEE Trans. on Image Processing*, 3(3):233–242, May 1994.

[17] R. Y. Tsai and T. S. Huang. Multiframe Image Restoration and Registration. In *Advances in Computer Vision and Image Processsing*, pages 317–339. JAI Press Inc., 1984.

[18] M. Turk and A. Pentland. Eigenfaces for Recognition. *J. of Cognitive Neuroscience*, 3(1):71–86, 1991.

[19] X. Wang and X. Tang. Hallucinating Face By Eigentransformation with Distortion Reduction. In *Proc. Int. Conf. on Biometrics Authentication*, Hong Kong, 2004.